

Excitation of Sn K - and L - and Ta L -shell x rays by 1.4–4.4-MeV protons

K. Ishii and S. Morita

Department of Physics, Tohoku University, Sendai, Japan

H. Tawara

Nuclear Engineering Department, Kyushu University, Fukuoka, Japan

H. Kaji and T. Shiokawa

Department of Chemistry, Tohoku University, Sendai, Japan

(Received 26 March 1974)

Excitation functions and absolute cross sections for Sn K - and L -shell and Ta L -shell x-ray production by proton impact have been measured over the energy range 1.4–4.4 MeV with a Si(Li) detector. The results, combined with our measurements on other elements, are compared with existing theories. In the calculation of ionization cross sections from the plane-wave Born approximation, we discuss the effect of a relativistic correction for the ionization potential. The plane-wave Born approximation with the correction due to the Coulomb deflection gives the best fit for Sn K x-ray production and the binary-encounter approximation is the best for Sn L and Ta L x-ray production. The semiclassical approximation based on the impact-parameter treatment predicts values which are not in agreement with the data on Sn L x rays. The scaled universal excitation curve based on the binary-encounter approximation gives good fits to K -shell ionizations but seems to show some disagreement for L -shell ionizations. The dependence of the $K\alpha/K\beta$ ratio of Sn on the target thickness was investigated but it was found that the ratio is constant within the experimental uncertainty. Relative intensities for the transitions $L\alpha$, $L\beta$, $L\gamma$, and L_i are also compared with the theories.

I. INTRODUCTION

Inner-shell ionization by heavy charged particles due to direct Coulomb interaction has been studied theoretically by Merzbacher and co-workers^{1,2} in terms of the plane-wave Born approximation (PWBA), by Garcia³ in terms of the binary-encounter approximation (BEA), and by Bang and Hansteen⁴ using the semiclassical approximation (SCA). Recently, modification of the PWBA has been developed by Basbas and co-workers^{5,6} by taking into account the effects of the Coulomb deflection of the projectile by the target nucleus and also of the increased binding energy of the target electrons induced by the presence of the projectile. The SCA calculation has been applied in the adiabatic energy region by Hansteen and Mosebekk.⁷

A number of experiments using thin targets have been done on K -shell ionization in these several years and the agreement between the theories and the observed total ionization cross sections is generally acceptable with variations being less than 30%.

In the theories recently developed by Hansen,⁸ Choi *et al.*,⁹ and McGuire and Richard,¹⁰ structure has been found in the L_1 -subshell-ionization cross sections, whereas L_2 - and L_3 -subshell-ionization cross sections are monotonically increasing functions of ion energy. However, measurements on L -shell ionization are still scarce. Recently,

Shafroth *et al.*¹¹ and Busch *et al.*¹² have reported the measurements on total x-ray production cross sections for the L shell of Au and Pb and also on the intensity ratios of $L\alpha$, $L\beta$, $L\gamma$, and L_i groups for these elements. Datz *et al.*,¹³ and Abrath and Gray¹⁴ have determined the absolute ionization cross sections for the L subshells of Au and Sm, respectively, by proton bombardment.

In this work, following our previous report¹⁵ on Zn K - and Pb L -shell ionization, the K - and L -shell ionizations for Sn and L -shell ionization for Ta have been studied for protons over the energy range 1.4–4.4 MeV. Partial cross sections and intensity ratios for the L x-ray groups have also been measured as a function of proton energy. Comparisons are made to the PWBA, BEA, and SCA calculations. Dependence of the $K\alpha/K\beta$ ratio for Sn on the target thickness has also been investigated.

II. EXPERIMENTAL PROCEDURE

The proton beam was accelerated by the 5-MV Van de Graaff generator at Tohoku University and was defined by a carbon slit of 3-mm diameter. Background x rays from the brass chamber wall due to scattered protons were reduced by a factor of 4 by coating the inner surface of the chamber with Aquadag. The self-supporting targets of 636- $\mu\text{g}/\text{cm}^2$ -thick Sn and 1.34-mg/cm²-thick Ta were

prepared by vacuum evaporation and rolling, respectively, and were mounted at 45° to the proton beam. An Ortec Si(Li) x-ray detector with a resolution of 205 eV at 5.9 keV was mounted at 90° to the beam outside the vacuum system and its effective solid angle was defined by a lead slit of 3-mm diameter. X rays passed through a 10- μ m Mylar window and 2.2-cm air path before entering the detector with a 25- μ m Be window. One or two 15- μ m aluminum absorbers were used to reduce the count rate due to the unresolved *M*-shell radiation. During the measurements, the count rate of the detecting system has been kept below 100 Hz in order to avoid a piling-up effect. To monitor the beam current and possible depletion of the targets, the elastically scattered protons were observed simultaneously with a surface-barrier silicon detector at 136° to the beam. It was confirmed that the proton scattering was Rutherford.

The solid angles were determined from the geometry to be 5.16×10^{-4} sr for the x-ray detector and 5.43×10^{-4} sr for the proton detector, respectively. The efficiency of the x-ray detector was determined using standardized x-ray emitting sources of ^{57}Co and ^{241}Am . Assuming that the x-ray production is isotropic and referring to the elastically scattered protons, the x-ray production cross section can be obtained from

$$\sigma_x = \left(\frac{d\sigma}{d\Omega} \right)_R \Delta\Omega_p \frac{4\pi N_x}{N_p \Delta\Omega_x \epsilon}, \quad (1)$$

where N_x is the number of counts in each peak of the x-ray spectrum corrected for the self-absorption in the target and absorption in the Mylar window, air, and aluminum absorber; ϵ is the efficiency of the x-ray detector; $(d\sigma/d\Omega)_R$ is the Rutherford scattering cross section; N_p is the number of counts in the back-scattered proton peak; $\Delta\Omega_x$ and $\Delta\Omega_p$ are the solid angles subtended by the x-ray and proton detectors, respectively.

In estimating the correction for absorption mentioned above, the photoabsorption cross sections for air and target materials were taken from a compilation of Storm and Israel.¹⁶ The absorption in the aluminum foil was measured experimentally. The energy loss of the incident beams in the targets was estimated to be 106–60 keV in the Ta target and 60–32 keV in the Sn target for 1.4–4.4-MeV protons.

Errors of the present measurements are estimated to be about 15%, including those of the detector efficiency (10%), the x-ray absorption (5%), and the solid angle (5%). Statistical errors are less than 2% for Sn *K*, Ta *L* α and *L* β x-rays, but varied from 5% to 25% for weaker groups of Ta *L* and Sn *L*.

III. RESULTS AND DISCUSSION

Typical spectra obtained are shown in Figs. 1(a)–1(c) for Sn *K*, Sn *L* and Ta *L* x rays, respectively. In Figs. 1(a) and 1(c), the groups are well separated, whereas smooth curves in Fig. 1(b) show peak separation by a least-squares-fitting program assuming Gaussian shapes and a linear background. Each peak is still a composite of several unre-

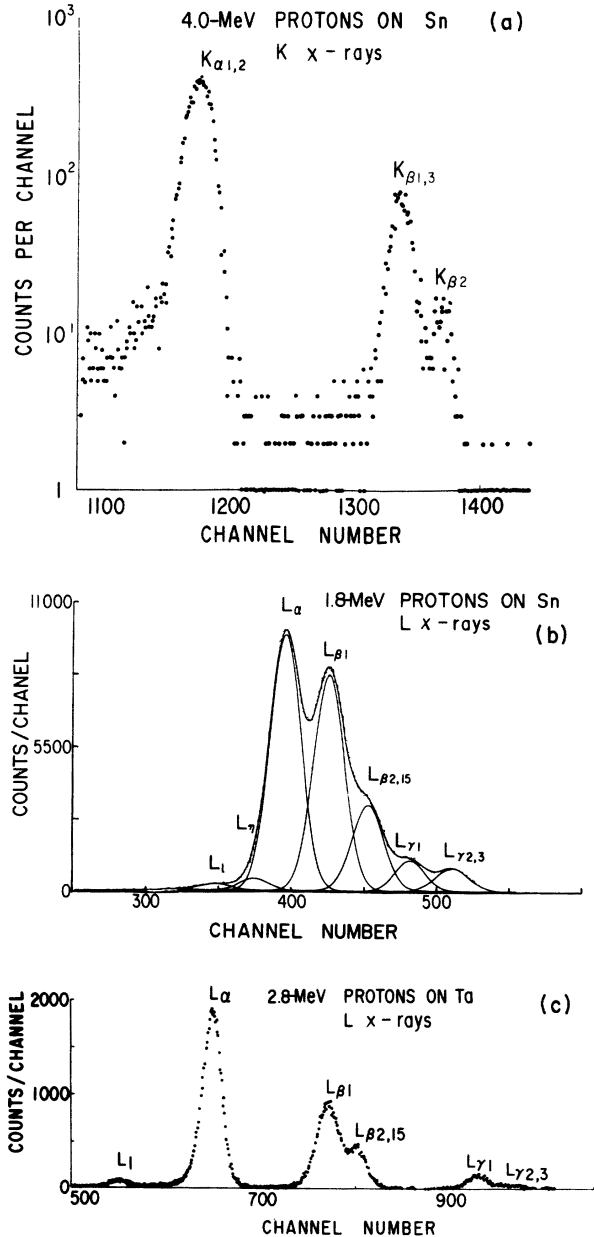


FIG. 1. (a), (b), and (c) Energy spectra of Sn *K* and *L* and Ta *L* x rays, respectively. Smooth curves in (b) show peak separation by a least-squares-fitting program assuming Gaussian shapes and a linear background.

solved lines because of the limited detector resolution.

A. Theoretical

The procedures to determine total and partial cross sections and x-ray intensity ratio and their comparisons to theories have been discussed previously.¹⁵ Briefly, the theoretical *L*-shell x-ray production cross section σ_x^L is related to the theoretical subshell ionization cross section σ_i^L , the subshell fluorescence yields ω , and the Coster-Kronig transition probabilities f by the formula

$$\sigma_x^L = \omega_1^{\text{eff}} \sigma_i^{L1} + \omega_2^{\text{eff}} \sigma_i^{L2} + \omega_3^{\text{eff}} \sigma_i^{L3}, \quad (2)$$

where

$$\omega_1^{\text{eff}} = \omega_1 + f_{12}\omega_2 + (f_{13} + f_{12}f_{23})\omega_3, \quad (3)$$

$$\omega_2^{\text{eff}} = \omega_2 + f_{23}\omega_3, \quad \omega_3^{\text{eff}} = \omega_3.$$

The values used for the fluorescence yields and the Coster-Kronig transition probabilities are taken from the work of Bambynek *et al.*¹⁷ The theoretical subshell-ionization cross sections are calculated from the BEA or PWBA. Concerning the *L*-subshell cross sections, the x-ray production cross sections are related to the ionization cross sections by the expressions,

$$\begin{aligned} \sigma_x^{L\alpha} &= [\sigma_i^{L1}(f_{13} + f_{12}f_{23}) + \sigma_i^{L2}f_{23} + \sigma_i^{L3}] \omega_3 \Gamma_{3\alpha} / \Gamma_3, \\ \sigma_x^{L\beta} &= [\sigma_i^{L1}(f_{13} + f_{12}f_{23}) + \sigma_i^{L2}f_{23} + \sigma_i^{L3}] \omega_3 \Gamma_{3\beta} / \Gamma_3 \\ &\quad + (\sigma_i^{L1}f_{12} + \sigma_i^{L2})\omega_2 \Gamma_{2\beta} / \Gamma_2 + \sigma_i^{L1}\omega_1 \Gamma_{1\beta} / \Gamma_1, \\ \sigma_x^{L\gamma} &= (\sigma_i^{L1}f_{12} + \sigma_i^{L2})\omega_2 \Gamma_{2\gamma} / \Gamma_2 + \sigma_i^{L1}\omega_1 \Gamma_{1\gamma} / \Gamma_1, \\ \sigma_x^{L\delta} &= [\sigma_i^{L1}(f_{13} + f_{12}f_{23}) + \sigma_i^{L2}f_{23} + \sigma_i^{L3}] \omega_3 \Gamma_{3\delta} / \Gamma_3, \\ \sigma_x^{L\eta} &= (\sigma_i^{L1}f_{12} + \sigma_i^{L2})\omega_2 \Gamma_{2\eta} / \Gamma_2, \end{aligned} \quad (4)$$

where the Γ 's are the radiative widths taken from the theoretical work of Scofield,¹⁸ which is based on the relativistic Hartree-Slater theory and includes the retardation effect.

Ionization cross sections calculated from the PWBA depend on the minimum energy transfer W_{min} . According to Merzbacher and Lewis,¹ W_{min} is equal to the effective ionization potential I_s , which is the solution of the (nonrelativistic) equation

$$-\frac{\hbar^2}{2m} \nabla^2 \psi_s - \frac{Z_s e^2}{r} \psi_s = (-I_s - V_s) \psi_s, \quad (5)$$

where Z_s is the effective nuclear charge taking into account the screening due to the inner shells, V_s is the screening potential due to the outer-shell electrons, and s is the principal quantum number. Then,

$$I_s = (Z_s^2/s^2)\mathcal{R} - V_s = I_{\text{NR}} - V_s, \quad (6)$$

where I_{NR} represents the nonrelativistic ionization potential neglecting the screening potential.

Similarly, we obtain the following equation from the relativistic treatment, which is necessary for heavy atoms,

$$I_0^i = I_R - V_s, \quad I_R = \frac{Z_s^2}{s^2} \left[1 + \frac{\alpha^2 Z_s^2}{s} \left(\frac{1}{j + \frac{1}{2}} - \frac{3}{4s} \right) \right] \mathcal{R}, \quad (7)$$

where I_0^i is the measured ionization potential, I_R is the solution of the relativistic equation [see Eq. (5)] and represents the relativistic ionization potential neglecting the screening potential, j is the total angular momentum number, α is the fine-structure constant, \mathcal{R} is the rydberg constant.

From Eqs. (6) and (7),

$$I_s = I_{\text{NR}} - I_R + I_0^i. \quad (8)$$

In the calculation of ionization cross sections from the PWBA, the parameter θ_s , often called the screening number and defined by $I_s = \theta_s I_{\text{NR}}$, is used for describing the binding energy. For the relativistic treatment,

$$\theta_s^A = \frac{I_0^i}{I_{\text{NR}}} - \frac{I_R - I_{\text{NR}}}{I_{\text{NR}}}. \quad (9)$$

Meanwhile, for the nonrelativistic case, $I_R \approx I_{\text{NR}}$ and then,

$$\theta_s^B = I_0^i / I_{\text{NR}}, \quad (10)$$

which is usually used for the PWBA calculations.

In the following discussions, the PWBA calculated by using θ_s^B , is represented by the PWBA-B and is compared with the PWBA-A, which uses θ_s^A [see Eq. (9)]. The values of θ_s , concerned here, are shown in Table I.

B. Excitation curves

The experimental and theoretical excitation curves for Sn *K* and *L* and Ta *L* x rays are shown in Figs. 2-4, respectively. As seen in these figures, the PWBA-A gives better fits than the PWBA-B for Sn *K* and *L*, and, especially, the

TABLE I. Values of θ_s .

		I_0^i (keV)	θ_s^A	θ_s^B	θ_s^A/θ_s^B	I_{NR}/I_R
Sn	<i>K</i>	29.2	0.836	0.869	0.96	0.97
	<i>L</i> ₁	4.465	0.589	0.624	0.94	0.97
	<i>L</i> ₂	4.156	0.546	0.581	0.94	0.97
	<i>L</i> ₃	3.929	0.542	0.549	0.99	0.99
Ta	<i>L</i> ₁	11.68	0.645	0.724	0.89	0.93
	<i>L</i> ₂	11.136	0.612	0.691	0.89	0.93
	<i>L</i> ₃	9.88	0.597	0.613	0.97	0.99

PWBA-A including the correction due to the Coulomb deflection is the best for Sn K .⁵ On the other hand, the PWBA-B is better than the PWBA-A for Ta L . This is contradictory to the fact that the relativistic effect is bigger for Ta than for Sn (see Table I). In order to improve this inconsistency, calculations would be desirable by using the relativistic wave function for L -shell electrons¹⁹ or by taking account of the perturbation of the target atomic states by the projectile.⁵ Corrections due to the Coulomb deflection for Sn L and Ta L x rays were estimated to be very small. Generally, the BEA calculation can reproduce best the experimental results, especially the change with energy, whereas the SCA curve for Sn L x rays deviates significantly from the others and gives values which are about one order of magnitude smaller than the experimental results at about 10 MeV.⁷

The over-all comparison of the experimental results, together with our measurements on other elements, with the scaled universal BEA curve is shown in Fig. 5, where the abscissa shows $E/\lambda U$ and the ordinate is $U^2\sigma$. Here, E is the bombarding energy of protons in keV, $\lambda=1836.1$ is the mass ratio of proton to electron, U is the binding

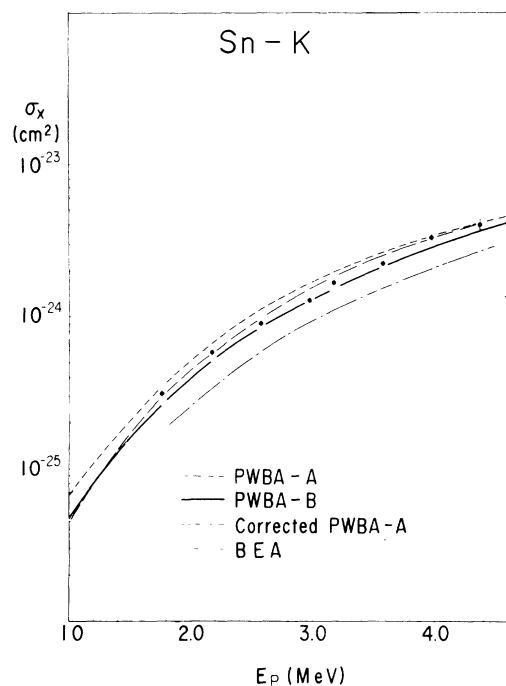


FIG. 2. Excitation curve for Sn K x rays. PWBA-A and -B are calculated using relativistic and nonrelativistic values of the ionization potential, respectively (see text). Corrected PWBA-A includes the correction due to the Coulomb deflection of incident protons.

energy of the electron in the target atom in keV, and σ is the ionization cross section. Regarding the L -shell ionizations, σ_i^{L1} , σ_i^{L2} , and σ_i^{L3} were estimated from the vacancy-production cross section given by Datz *et al.*,¹³ neglecting the intensities of σ_x^{L1} and σ_x^{L2} , and only the σ_i^{L3} are shown, as σ_i^{L1} and σ_i^{L2} are small and their errors large. In this figure are also shown the Au M -shell-ionization cross sections, details of which will be published in a separate paper. The absolute cross sections of Au M -shell ionization have considerably large uncertainty because of the ambiguity of the fluorescence yields for these shells¹⁷ and of the corrections for detector efficiency and absorption for these low-energy x rays.

It must be noted that the σ^{L3} and σ^M show somewhat different behavior from the universal curve, though the K -shell ionizations are generally in good agreement with the BEA curve. This fact might be due to the difference in spacial distribution of the wave functions for different shells which gives rise to different behavior of the overlapping integral.

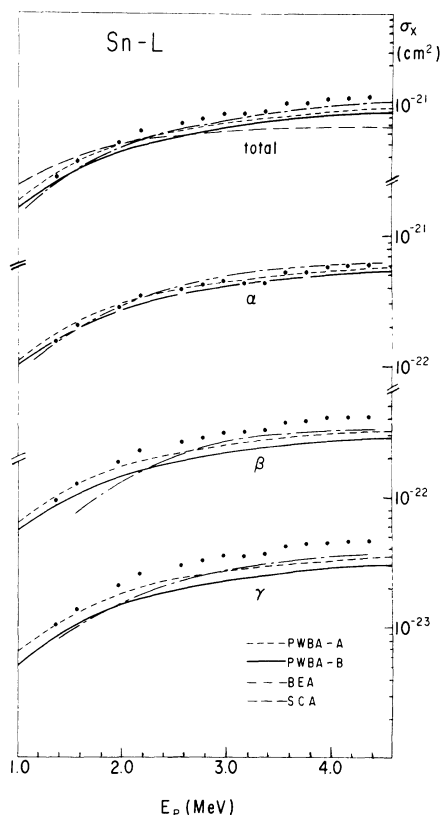


FIG. 3. Excitation curves for Sn L x rays. SCA is the semiclassical approximation. The notations are the same as in Fig. 2.

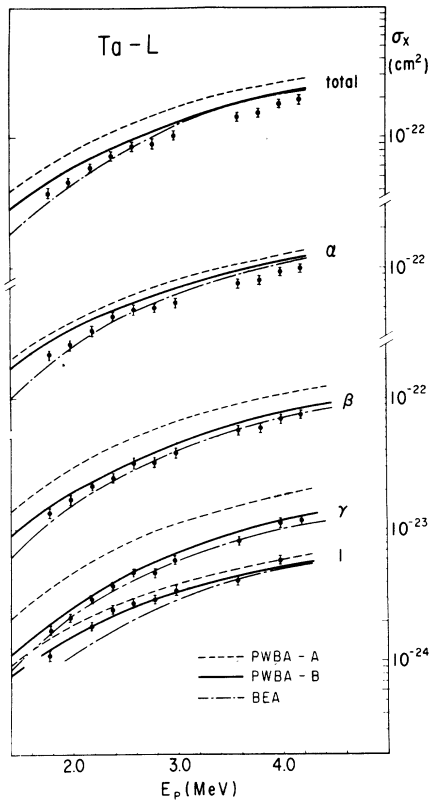


FIG. 4. Excitation curves for Ta L x rays. Same as in Fig. 2.

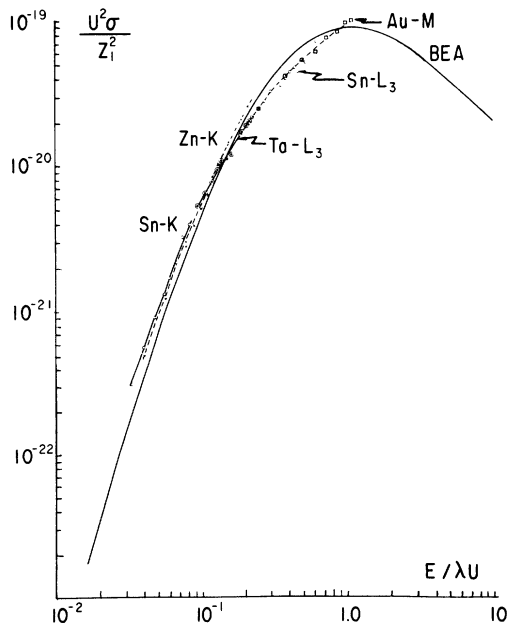


FIG. 5. Comparisons of the experimental excitation curves with the scaled universal curve of the BEA.

TABLE II. Comparison of $K\alpha/K\beta$ for Sn in experiments and theory.

	$K\alpha/K\beta$	Excitation
present	4.41	proton
Hansen <i>et al.</i> ²⁰	4.49	radioisotope
Hardt-Watson ²¹	4.545	α particle
Mistry-Quarles ²²	4.68	electron
Middleman <i>et al.</i> ²³	4.61	electron
Close <i>et al.</i> ²⁴	4.46	proton
Scofield ¹⁸	4.89	theory

C. X-ray production ratios

In theoretical calculations of the x-ray production ratios, the effects of the Coulomb repulsion of the projectile by the target nucleus are cancelled out or at least reduced. From an experimental point of view, many uncertainties, such as the inhomogeneity of target thickness and uncertainty in the geometry, are eliminated. Therefore, the experimental values of the ratio provide a more rigorous test for theoretical calculations.

The $K\alpha/K\beta$ ratio for Sn was obtained after correction for absorptions and for the x-ray detection efficiency and was found to be 4.41 and is constant within the experimental errors of ± 0.11 , independently of the projectile energy. A comparison of the ratio $K\alpha/K\beta$ obtained from various experiments²⁰⁻²⁴ and from the theoretical calculation of Scofield¹⁸ is given in Table II. The present value is consistent with those obtained by Hansen *et al.*²⁰ using a carrier-free radioisotope, by Hardt and Watson²¹ using 30-80-MeV α particles and by Close *et al.*²⁴ using protons. However, it is a little less than those obtained by Mistry and

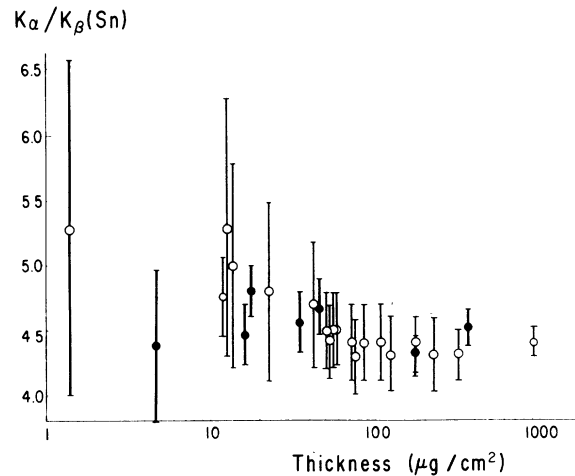


FIG. 6. Thickness effect of $K\alpha/K\beta$ ratio of Sn. Closed circles, present results; open circles, Mohler-Cothren results. The theoretical value of the ratio is 4.89.

Quarles²² with 120-keV electron bombardment and by Middleman *et al.*²³ with several-hundred-MeV electron bombardment. The theoretical value of Scofield is still higher (10%) than the experimental results. It is generally expected that, in the case of proton bombardment, the effect of simultaneous outer-shell ionization on the $K\alpha/K\beta$ ratio would be small.

As in this case, the experimental values of $K\alpha/K\beta$ ratio for medium Z elements are consistently lower than the theoretical values by (10–20)%. Recently, Mohler and Cothorn²⁵ have

reported that the $K\alpha/K\beta$ ratio of tin depends on the sample thickness. For very thin samples, the ratio seems to agree with the theoretical value and this effect could be due to the surface effects involving different bonding of the L and M levels, or the nonuniform distribution of tin could produce a differential charging effect. To check this thickness effect on the $K\alpha/K\beta$ ratio, Sn targets of various thickness evaporated on 10- μ m Mylar were bombarded with 3.5-MeV protons. The thickness of tin was determined from the Rutherford scattering of protons. Our results on this effect are shown in Fig. 6, together with those of Mohler

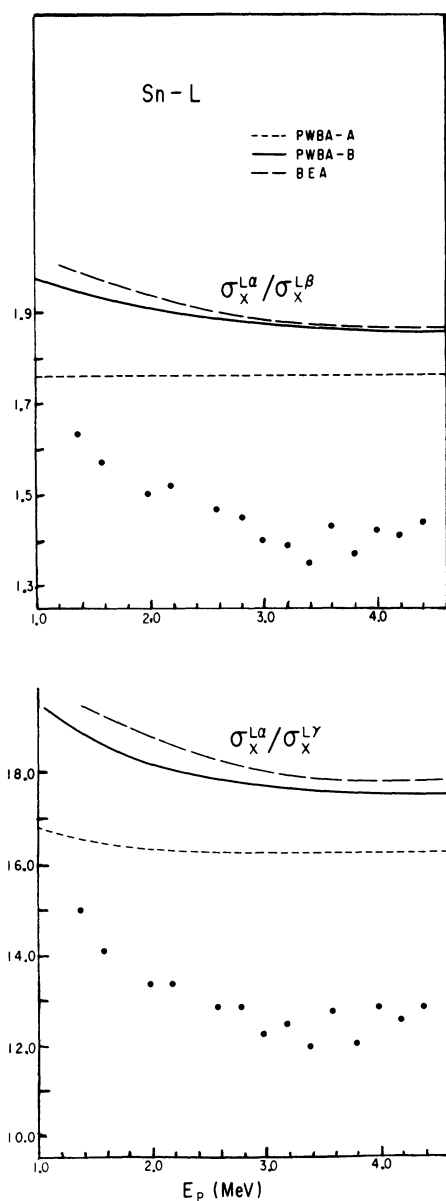


FIG. 7. $L\alpha/L\beta$ and $L\alpha/L\gamma$ ratios for Sn L x rays. Same notations for the theoretical curves as in Fig. 2.

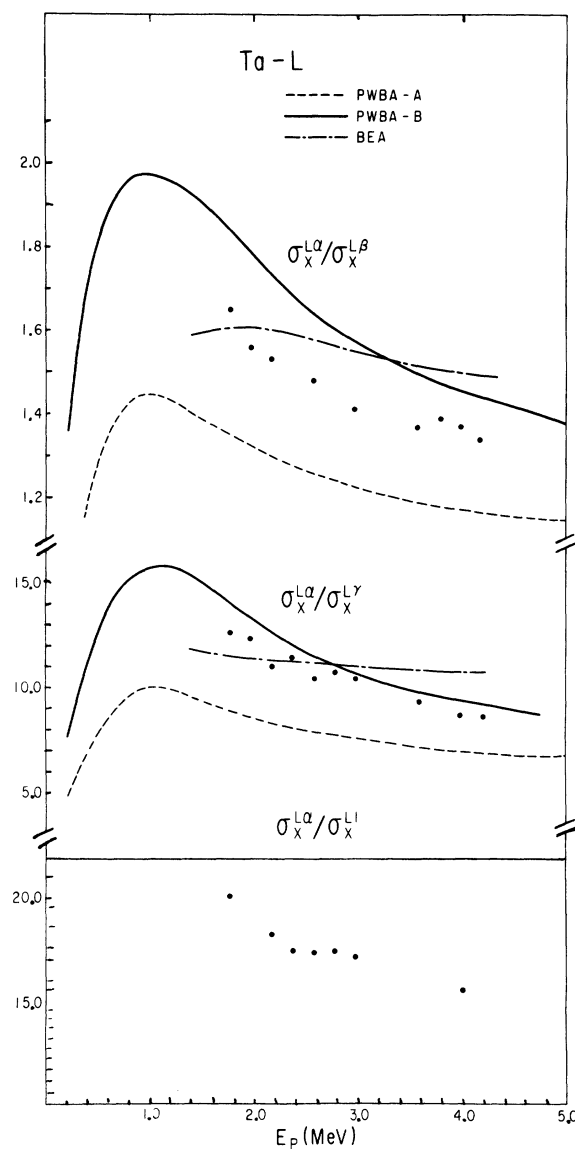


FIG. 8. $L\alpha/L\beta$, $L\alpha/L\gamma$, and $L\alpha/L_I$ ratios for Ta L x rays. Same notations for the theoretical curves as in Fig. 2. The theoretical $L\alpha/L_I$ ratio is constant.

and Cothorn, where the bremsstrahlung from ^{147}Pm was used for the x-ray excitation. Contrary to their results, no evidence for the thickness effect was found in our case.

Intensity ratios of $L\alpha/L\beta$, $L\alpha/L\gamma$, and $L\alpha/L_1$ for Sn and Ta are shown in Figs. 7 and 8, respectively, as a function of proton energy. Theoretical values from the PWBA and BEA are also shown. The difference between the PWBA-B and BEA is not so great for Sn and the PWBA-A is the closest to the experimental results. For Ta, the experimental values lie between the PWBA-A and -B and are closest to the BEA. The theoretical $L\alpha/L_1$ ratio is independent of proton energy, as these two transitions originate from the filling of a hole in the L_3 subshell exclusively. On the other hand, the ratio for Ta is energy dependent and this might be due to the effect of multiple ionization.

IV. SUMMARY

Productions of Sn K and L and Ta L x rays by proton impact have been measured over the energy

range 1.4–4.4 MeV. $K\alpha/K\beta$, $L\alpha/L\beta$, $L\alpha/L\gamma$, and $L\alpha/L_1$ ratios have also been measured. The results are compared with the PWBA, BEA, and SCA calculations. The SCA does not agree with the experimental results for Sn L x-ray production. In the PWBA calculation, the effect of relativistic correction for the electron binding energy is discussed. Though the K -shell-ionization cross sections are well described with the BEA, some deviations from the scaled universal curve of the BEA are found for the L -shell ionizations. Thickness effect on the $K\alpha/K\beta$ ratio of tin was investigated, but no evidence was found. Contrary to the theoretical prediction, an energy dependence of $L\alpha/L_1$ ratio for Ta was observed.

ACKNOWLEDGMENTS

The authors are grateful to M. Kato for the skillful operation of the Van de Graaff generator during this work.

-
- ¹E. Merzbacher and H. W. Lewis, *Encyclopedia of Physics*, edited by S. Flügge (Springer-Verlag, Berlin, 1958), Vol. 34, p. 166.
- ²G. S. Khandelwal, B. H. Choi, and E. Merzbacher, *At. Data* **1**, 103 (1969); V. B. H. Choi, PWBA calculations (unpublished).
- ³J. D. Garcia, *Phys. Rev. A* **1**, 280 (1970); *Phys. Rev. A* **1**, 1420 (1970).
- ⁴J. Bang and J. M. Hansteen, *Mat. Fys. Medd. Dan Vid. Selsk.* **31**, No. 13 (1959).
- ⁵G. Basbas, W. Brandt, and R. Laubert, *Phys. Rev. A* **7**, 983 (1973).
- ⁶G. Basbas, W. Brandt, and R. H. Ritchie, *Phys. Rev. A* **7**, 1971 (1973).
- ⁷J. M. Hansteen and O. P. Mosebekk, *Nucl. Phys. A* **201**, 541 (1973).
- ⁸J. S. Hansen, *Phys. Rev. A* **8**, 822 (1973).
- ⁹B. H. Choi, E. Merzbacher, and G. S. Khandelwal, *At. Data* **5**, 291 (1973).
- ¹⁰J. H. McGuire and P. Richard, *Phys. Rev. A* **8**, 1374 (1973).
- ¹¹S. M. Shafroth, G. A. Bissinger, and A. W. Walther, *Phys. Rev. A* **7**, 566 (1973).
- ¹²C. E. Busch, A. B. Baskin, P. H. Nettles, and S. M. Shafroth, *Phys. Rev. A* **7**, 1601 (1973).
- ¹³S. Datz, J. L. Duggan, L. C. Feldman, E. Laegsgaard, and J. U. Andersen, *Phys. Rev. A* **9**, 192 (1974).
- ¹⁴F. Abrath and T. J. Gray, *Phys. Rev. A* **9**, 682 (1974).
- ¹⁵H. Tawara, K. Ishii, S. Morita, H. Kaji, C. N. Shu, and T. Shiokawa, *Phys. Rev. A* **9**, 1617 (1974).
- ¹⁶E. Storm and H. I. Israel, *Nucl. Data A* **7**, 565 (1970).
- ¹⁷W. Bambynek, B. Crasemann, R. W. Fink, H. L. Freund, H. Mark, C. D. Swift, R. E. Price, and P. Venugopala Rao, *Rev. Mod. Phys.* **44**, 716 (1972).
- ¹⁸J. H. Scofield, *Phys. Rev.* **179**, 9 (1969).
- ¹⁹B. H. Choi, *Phys. Rev. A* **4**, 1002 (1971).
- ²⁰J. S. Hansen, H. U. Freund, and R. W. Fink, *Nucl. Phys. A* **142**, 604 (1970).
- ²¹T. L. Hardt and R. L. Watson, *Phys. Rev. A* **7**, 1917 (1973).
- ²²V. D. Mistry and C. A. Quarles, *Nucl. Phys. A* **164**, 219 (1971).
- ²³L. M. Middleman, R. L. Ford, and R. Hofstadter, *Phys. Rev. A* **4**, 1429 (1970).
- ²⁴D. A. Close, R. C. Bearse, J. J. Malanify, and C. J. Umbarger, *Phys. Rev. A* **8**, 1873 (1973).
- ²⁵R. E. Mohler and C. R. Cothorn, *Nucl. Instrum. Methods* **113**, 599 (1973).